

Combining Fluorescent Cell Barcoding and Flow Cytometry-based Phospho-ERK1/2 Detection at Short Time Scales in Adherent Cells

Sonal Manohar,[†] Prachi Shah,[†] Sharmila Biswas,[†] Anam Mukadam, Madhura Joshi, Ganesh Viswanathan*

Department of Chemical Engineering,
Indian Institute of Technology Bombay,
Powai, Mumbai 400076, India

Received 21 June 2018; Revised 9
August 2018; Accepted 20 August 2018

Grant sponsor: Science and Engineering
Research Board (SERB), Department of
Science and Technology, Government
of India, Grant number: SB/S3/
CE/048/2014

Additional Supporting Information may
be found in the online version of this
article.

*Correspondence to: Ganesh Viswa-
nathan, Department of Chemical Engi-
neering, Indian Institute of Technol-
ogy Bombay, Powai, Mumbai 400076, India
Email: ganeshav@iitb.ac.in

[†]These authors contributed equally.

Published online 2 October 2018 in
Wiley Online Library
(wileyonlinelibrary.com)

DOI: 10.1002/cyto.a.23602

© 2018 International Society for
Advancement of Cytometry

• Abstract

Detection of levels of intracellular phospho-proteins is key to analyzing the dynamics of signal transduction in cellular systems. Cell-to-cell variability in the form of differences in protein level in each cell affects signaling and is implicated in prognosis of many diseases. Quantitative analysis of such variability necessitate measuring the protein levels at single-cell resolution. Single-cell intracellular protein abundance detection in statistically significant number of adherent cells for short time sampling points post stimulation using classical flow cytometry (FCM) technique has thus far been a challenge due to the detrimental effects of cell detachment methods on the cellular machinery. We systematically show that cell suspension obtained by noninvasive temperature-sensitive detachment of adherent cells is amenable to high-throughput phospho-ERK1/2 protein detection at single-cell level using FCM in these short time sampling points. We demonstrate this on three adherent cell lines, viz., HeLa, A549, and MCF7, from distinct lineages having characteristically different elasticity at 37 °C. In particular, we use a right combination of multiplexing via fluorescent cell barcoding (FCB) and intracellular antibody staining for simultaneous detection of phospho-ERK1/2 (pERK) stimulated by epidermal growth factor (EGF) in multiple samples. Based on systematic characterization using Alexa 350 dye, we arrive at two conditions that *must* be satisfied for correct implementation of FCB. Our study reveals that the temperature-sensitive detachment of HeLa cells correctly captures the expected pronounced bimodal pERK distribution as an early response to EGF, which the enzymatic treatment methods fail to detect. © 2018 International Society for Advancement of Cytometry

• Key terms

adherent cells; phosphoflow; intracellular staining; short time scale sampling; fluorescent cell barcoding; flow cytometry

POPULATION average measurements, popularly used in laboratory and clinical settings, reflect only representative behavior of an ensemble of heterogeneous cells and, therefore, fail to distinguish variable signaling dynamics within single cells (1). However, existence of cell-to-cell variability has been demonstrated in an ensemble of primary (normal (1) and diseased (2)) and immortalized cells (3–5). Use of variability in protein levels that quantitatively reflect the inherently present cellular heterogeneity for various analysis and detection purposes can offer significant insights into the underlying principles (6–10). Capturing this variability in protein levels requires detection at single-cell level in statistically significant number of cells, which is currently a routine practice in case of those cells cultured in a suspension. However, most tissues being adherent in nature, these approaches are not directly applicable to such type of cells. Clearly, there is a need for a reliable method for capturing the protein levels at single-cell level in an ensemble of adherent cells.

Single-cell analysis of adherent cells is historically carried out by methods based on immunofluorescence microscopy, which is unsuitable for detection in statistically significant number of cells. Moreover, multiplexing of microscopy-based assays demands extensive manipulation steps making it low-throughput (11). While flow cytometry (FCM)-based methods offer detection in statistically large numbers (millions of cells) (12), permit multiparameter detection (6) and relatively easy multiplexing (13), and are amenable to studying phenotypic variability (14), it requires cells to be in a suspension.

Release of individual adherent cells from the substrate while preserving the surface receptor activity and intracellular signaling machinery is a challenge. Currently available isolation methods such as mechanical scraping (15) and enzymatic treatment using trypsin/chelators (16–18) hamper the cell health and the signal flow to key proteins (markers) such as those in MAPK cascades possibly due to damage of cell-surface receptors. Moreover, these methods, if signal preserving for certain cell types, are well-suited only for long time-scale measurements, wherein the sampling time is much larger than that for the detachment process itself. Recently, a fitting combination of mechanical forces and biochemical treatment method for the detachment of adherent cells led to preservation of the gene expression at single-cell level (15,19). These combination methods are promising. However, due to the use of enzyme treatment, the extent of preservation of the receptor expression and therefore downstream signal is likely to be context—cell line and stimulus—specific.

FCM-based detection of levels of activated ERK (pERK), an important marker for cancer (5), and other phosphoproteins in various suspension cells is routinely carried out (8,20–23). Recently, FCM-based detection of intracellular phospho-protein levels such as that of pERK and pAkt in primary/immortalized adherent cells was attempted after detachment, post-stimulation, using trypsinization in ice-cold conditions (16,24) or at room temperature (RT) with (24)/without (25,26) sample multiplexing. While simultaneous cell detachment and brief arresting of signaling via ice-cold trypsinization are viable options for cells used in these studies, its applicability is cell-type specific and it often may need placing cells overnight under cold conditions, which may be undesirable (18). Therefore, for stimulated cells detached using ice-cold trypsinization, time-lag between stimulation and cell fixation, which guarantees arresting the signaling process, is imminent making cells unsuitable for short-time scale sampling of activated proteins.

Given the potential limitations of the existing approaches for high-throughput, flow cytometric protein level detection in adherent cells at short-time scales, in this study, we propose an alternative approach for this purpose. Specifically, we demonstrate the possibility of reliable phospho-ERK1/2 response preserving cell detachment using thermally induced noninvasive method (27–29) and stimulation post detachment, which enables instantaneous fixation of the cells at the desired short-time scale sampling points. We systematically show that such isolated cells are amenable to both stimulation post detachment and FCM-based multiplexing assays such as fluorescent

cell barcoding (FCB). We assess the suitability of the proposed approach for simultaneous multiplexing of samples and its reliability for short timescale measurement of pERK levels in the ensemble of adherent cells by systematic experimentation on three adherent cell lines from distinct lineages possessing characteristically different adhesion properties.

MATERIALS AND METHODS

Cell Culture, Reagents, and Detachment

HeLa, A549, and MCF7 cells were procured from Cell Repository at National Centre for Cell Science (NCCS, Pune, India). HeLa and MCF7 were cultured in DMEM and A549 in RPMI-1640, both the media containing 10% fetal bovine serum (FBS), 2 mmol/l L-glutamine, 1% antibiotic-antimycotic solution, all procured from HiMedia (Mumbai, India). Cells were maintained at 37°C in a humidified 5% CO₂ incubator. While epidermal growth factor (EGF) (Sigma, St. Louis, MO, USA) was reconstituted in double-distilled water, Phorbol 12-myristate 13-acetate (PMA) (Sigma) was dissolved in DMSO. In both cases, following reconstitution to a concentration of 1 mg/ml, the stock was stored at –20°C until use and diluted in PBS before treatment. Cell detachment using trypsin and accutase was achieved using standard methods (30,31). In contrast, cells cultured in temperature-sensitive Nunc™ multidishes with UpCell™ surface (UpCell plates) (Thermo Fisher Scientific, Waltham, MA, US) were detached by placing the plates at 20°C for 15 min followed by rigorous mixing (32). Cells were then collected, pelleted by centrifugation at 1,000 rpm for 5 min at RT, equilibrated in complete media at 37°C for 30 min and washed once with PBS before further use.

Annexin V/PI Staining

Harvested cells were washed once with PBS, resuspended in 1X Annexin binding buffer and stained with FITC-labeled Annexin V and PI (BD Pharmingen, San Diego, CA, US). Cells were analyzed on BD FACS Aria™ within 30 min (BD Biosciences, San Jose, CA, US).

Western Blotting

For direct lysis, cells in the monolayer in regular six-well plates (not exposed to detaching agents) were stimulated, washed, and prepared for lysis. In contrast, accutase/UpCell-detached cells, after stimulation, were washed twice with PBS and pelleted. Cells were lysed by resuspending pellets of detached cells or gently mechanically scraped cell monolayer into CelLytic™ M buffer (Sigma) containing protease inhibitor cocktail (Sigma) and Halt™ phosphatase inhibitor cocktail (Thermo Fisher Scientific) and incubated for 1 h at 4°C with intermittent vortexing. Cell lysates were then centrifuged at 13,000 rpm for 20 min at 4°C. Bradford reagent and bovine serum albumin (BSA) (HiMedia, Mumbai, India), as a standard, were used for the estimation of protein content in supernatant on SpectraMax® M5 plate reader (Molecular Devices, San Jose, CA, US). A total of 30–40 µg total protein from each sample was subjected to immunoblotting. Blot was probed with specific antibody to phospho-ERK1/2 (T202/

Y204) (clone 20A) or anti-ERK clone 16 (pan ERK) (BD Biosciences) and then with HRP-conjugated anti-mouse IgG (Santa Cruz Biotechnology, Dallas, TX). Specific proteins were detected using Clarity ECL western blotting substrate (Bio-Rad, Hercules, CA), and blots were imaged on Geliance 2000 system (Perkin Elmer, Waltham, MA, US). Densitometric analysis of the blot images was done using ImageJ (33).

Intracellular Staining of pERK

Cells (unstimulated or stimulated with EGF/PMA post detachment) were fixed with 2% (HeLa) or 4% (A549 and MCF7) PFA for 10 min at RT, washed once with PBS, permeabilized with 500 μ l of 90% chilled methanol on ice, and washed with 0.5% BSA in PBS to remove leftover methanol. Cells resuspended in staining medium (0.02% saponin + 0.5% BSA in PBS) were stained with phospho-ERK1/2 (T202/Y204) (clone 20A)-Alexa 488-tagged antibody (BD Biosciences) or p44/42 MAPK (ERK1/2)-(clone 137F5)-Alexa 488-tagged antibody (Cell Signaling Technology, Danvers, MA). After removing unbound antibody, cells resuspended in 300 μ l of 0.5% BSA containing 1% PFA (for crosslinking antigen-antibody) were analyzed on flow cytometer. Post acquisition, after automated gating using FlowPeaks (34) clustering technique implemented in R-Studio (version 3.4.0), raw fluorescence was rescaled into molecules of equivalent fluorescence (MEF) using FlowCal (35) and the data were analyzed using FlowJo[®] (version 10). For calculating MEF, rainbow calibration particles (8 peaks, 3.0–3.4 μ m) (Sphero[™]; BD Biosciences) were used for calibration of the FITC channel, in which Alexa 488 fluorescence is detected.

Fluorescent Cell Barcoding

Detached cells were suspended in PBS and divided into four tubes. Cells were fixed and permeabilized using the procedure specified in the method for “Intracellular staining of pERK.” Samples in four different tubes were *barcoded* with those many different concentrations of Alexa fluor[®] 350 (excitation: 346 nm, emission: 442 nm) or Alexa fluor[®] 647 (excitation: 650 nm, emission: 665 nm) NHS ester dye (Thermo Fisher Scientific) and incubated for 40 min on ice. After washing first with PBS, followed by three washes with 0.5% BSA, and then by PBS, cells in individual tubes were centrifuged. Two-thirds (by volume) of the resuspended barcoded sample from each tube were combined into a single *combo-tube*, and the remaining in each of them was retained as a *single-tube* control. After washing the pelleted cells in combo-tube with 0.5% BSA, cells resuspended in 500 μ l of 0.5% BSA were analyzed on BD FACS Aria[™]. Post acquisition, data were analyzed on FlowJo[®] (version 10) after automated gating and deconvolution using FlowPeaks clustering in R-Studio (34).

Intracellular Staining of EGF/PMA-Induced pERK in Barcoded Samples

Cells, stimulated as above or unstimulated, were first barcoded, as detailed in method for “FCB,” to obtain a combo-tube. Barcoded sample in the combo-tube was stained

with phospho-ERK1/2-Alexa 488-tagged antibody, washed as mentioned earlier, and analyzed on BD FACS Aria[™]. (Total ERK staining was done for unstimulated or EGF stimulated cells as mentioned above.) Post acquisition, after automated gating and cluster deconvolution as specified in method for “FCB” and rescaling raw fluorescence to MEF, the data were subsequently analyzed on FlowJo[®] (version 10).

Statistical Analysis of pERK Activation

Student’s paired *t*-test was performed on autofluorescence (double negative) corrected median fluorescence intensity (MFI) of pERK normalized with corresponding average (autofluorescence corrected) MFI for total ERK for stimulated and unstimulated cells (negative control) (Microsoft Office 2007). Differences between the groups with $P < 0.05$ were considered statistically significant. Note that the averaging for corrected MFI of total ERK levels is across technical replicates and the resulting average is different for each of the stimulation conditions.

RESULTS

Temperature-Sensitive Physical Detachment of Cells

In this study, in order to preserve the health and the signaling properties, we consider the use of UpCell culture plates that offers temperature-sensitive cell detachment. As model cell lines, we use cells from different cancer lineages, viz. HeLa (cervical adenocarcinoma), A549 (lung epithelial carcinoma), and MCF7 (breast adenocarcinoma). Mean Young’s modulus reflecting elasticity or stiffness, which impacts the detachment process at culture conditions, that is, 37°C, for these three cell lines estimated from the cell stiffness distribution reported in Li et al. (36) is 4.18, 2.03, and 2.55 kPa. While HeLa and MCF7 display variation in elasticity as a response to decrease in temperature (mean Young’s modulus of 2.49 and 2.67 kPa, respectively, at 25 °C (36)), Young’s modulus of A549 cells is relatively insensitive to temperature changes (2.12 kPa at 25°C). While MCF7 cells at RT (25°C) are marginally softer than that at 37°C, stiffness of HeLa cells increases with a decrease in temperature from 37°C to RT. Note that at both temperatures, MCF7 cells display a bimodal stiffness distribution with the two modes, respectively, having Young’s modulus in the range (~1.29, ~2.55) and (~2.55, ~4.42) in kPa (36).

We first assess the effect of temperature-sensitive detachment of the three cell lines on the overall cell health by comparing the cell viability with that achieved using the standard trypsinization and accutase treatment. (For the sake of brevity, Temperature-sensitive, Accutase treatment, and Trypsinization-based Cell Detachment methods will henceforth be referred to as TeCD, AcCD, and TrCD methods, respectively.) Figure 1 shows the fraction of viable HeLa cells and those in different phases of cell death (detected using Annexin-PI staining [“Materials and methods” section]) for the three detachment methods. (Such a comparison for A549 and MCF7 cells is in Supporting Information Figure S1.) The fraction of population distributed in necrotic/apoptotic stages

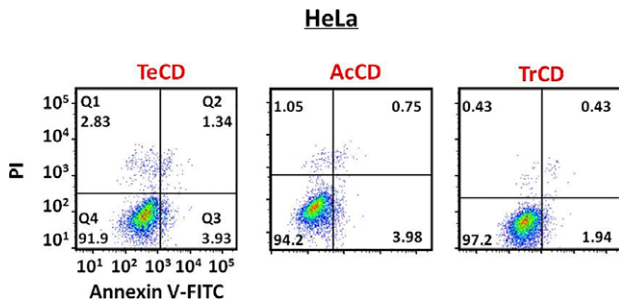


Figure 1. Cell viability using temperature-sensitive detachment and enzyme-based detachment was obtained using flow cytometry. Assessment of cell viability was done using Annexin V–PI assay after using temperature sensitive (TeCD) or enzymatic (accutase: AcCD or trypsin: TrCD) detachment methods on HeLa cells ($n = 3$). Fraction of live and dead cells gated in different quadrants: Q1—necrotic, Q2—late apoptotic, Q3—early apoptotic, and Q4—live cells. [Color figure can be viewed at wileyonlinelibrary.com]

(quadrants 1–3) is $< \sim 10\%$ in all the cases. Thus, viability of all three adherent cell lines released from substrate using TeCD, when compared with those with other two treatments is reasonable.

Intracellular Staining of Adherent Cells Stimulated with EGF: Single-Cell pERK Levels

We next ask a question if these detachment methods preserve the pERK response in the released cells and are amenable for phospho-ERK1/2 estimation using FCM. Detection of key signaling marker pERK in cells stimulated using EGF is widely used as a model for single-cell level studies (5,26). In this study, we primarily consider pERK response to EGF stimulation. Since pERK response is known to be stimulus-specific (37), we also present pERK response to synthetic activator Phorbol-12-myristate 13-acetate (PMA), which is also used as a model stimulant in various laboratory studies (16).

pERK activation and the underlying signaling dynamics being cell-line specific (38), before FCM-based detection is considered, we assess if the chosen cell lines indeed exhibit pERK activation as a response to EGF stimulation. For this, we detect, using western blotting (“Materials and methods” section), average pERK and total ERK (tERK) in (1) stimulated cells followed by direct lysing and (2) cells detached using the TeCD and AcCD methods followed by stimulation. In each of these cases, cells were stimulated with 100 ng/ml EGF for 5 min. In Figure 2A-i, we present the pERK and total ERK blots for the case of cells stimulated and then directly lysed. Blot images for pERK levels in all three cell lines detached using TeCD and AcCD and stimulated with EGF are in Figure 2A-ii, with the fold change (normalized with the corresponding tERK levels) estimated using densitometry (“Materials and methods” section) in Supporting Information Figure S2A. pERK levels estimated at 5 min post stimulation for the case of HeLa and A549 detached using TeCD or AcCD qualitatively match well with that for the case of direct lysis. However, for the case of MCF7, darker bands indicating higher pERK levels were found for the case of direct lysis.

AFM studies on MCF7 cells display bimodal Young’s modulus distribution, that is, fraction of cells in a population possesses higher Young’s modulus than the rest (36). Since shear stress due to even gentle mechanical scraping can cause rapid activation of pERK in certain cells (39), a fraction of the lysed MCF7 cells could be expressing higher pERK resulting in an overall darker band in the immunoblots. Distinct pERK bands at the chosen time points for direct lysis and the bands and the fold change for TeCD and AcCD suggest that clearly all three cell lines display pERK response to the chosen stimulation. Since the pERK response is stimulus specific (37), we show the same when cells were stimulated using 1 $\mu\text{g/ml}$ PMA for 15 min and contrast these with the corresponding western blots (Supporting Information Fig. S3A).

We next show that FCM-based detection of pERK levels in the chosen adherent cell lines is possible. We stimulate the isolated cells in suspension with 100 ng/ml EGF for 5 min. In Figure 2B, we show the normalized histograms (or probability distribution) of the pERK levels for negative control and EGF-treated samples for HeLa, A549, and MCF7 for TeCD, AcCD, and TrCD methods. (Replicates are in Supporting Information Fig. S2B.) Shift in the histograms of pERK for the stimulated conditions suggests that activation is indeed detected in an ensemble of cells for all the three model cell lines for all three detachment methods. Supporting Information Figure S3B shows pERK level detection using FCM for the case of PMA stimulation (1 $\mu\text{g/ml}$ for 15 min) as well. While the activation indicated by the shift, trend of which is similar to that detected using immunoblotting, that is, population-averaged measurements, for the case of TeCD and AcCD, is comparable across all three detachment methods for the three cell lines used, a small variation in the spread of the distribution is observed in the case of the TeCD. Moreover, pronounced bimodal distribution was achieved in the case of HeLa and MCF7 cells *only* while using TeCD. Recent time-lapse microscopy study showed that such pronounced pERK bimodal distribution is expected at short time scales for HeLa cells stimulated with EGF (5).

Adherent Cells Detached Using TeCD Suitable for Multiplexing Using FCB

Multiplexing of FCM assays using FCB offers a unique advantage of simultaneous circumvention of the flow cytometer machine introduced noise and possible reduction in the quantity of (often expensive) reporter (antibody) required (13). FCB involves embedding unique signatures in the form of distinct dye concentrations in different samples before combining them for high-throughput experimentation. Such a multiplexing strongly hinges on the ability to deconvolute the individual sample clusters post acquisition based on the separation witnessed in the corresponding fluorescence emitted by them. This could be cell-type and barcoding dye specific and influenced by the detachment technique. Moreover, the multiplexing assays require multiple washing steps, that is, centrifugation, which may cause additional stress over and above that by the detachment process itself. In order to assess the suitability of the chosen adherent cell lines for such a

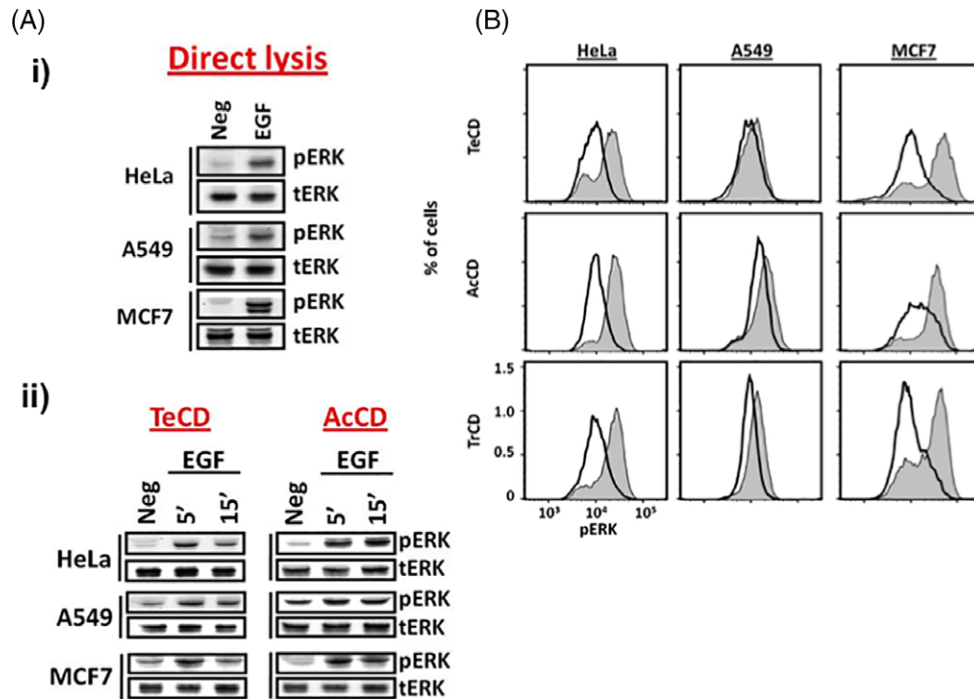


Figure 2. (A) Levels of phospho ERK (pERK) and total ERK (tERK) in unstimulated and stimulated cells for the three adherent cell lines obtained using western blotting ($n = 2$). (i) Cells stimulated with EGF (100 ng/ml) for 5 min followed by direct lysis. (ii) Cells were detached by TeCD or AcCD followed by EGF stimulation (100 ng/ml for 5 or 15 min). (B) Comparison of pERK distribution (obtained by flow cytometry) in cells detached using temperature-sensitive method (TeCD) and accutase treatment (AcCD) and trypsinization (TrCD) ($n = 3$, replicates are shown in Supporting Information Fig. S2B). Unfilled histograms: unstimulated and stained (negative control) and gray histograms: EGF (100 ng/ml, 5 min). [Color figure can be viewed at wileyonlinelibrary.com]

high-throughput FCM experimentation, we next considered FCB on these cells using Alexa Fluor[®] 350 dye (“Materials and methods” section).

A comparison of the barcoded clusters obtained using TeCD (Fig. 3A-i) with those obtained using AcCD or TrCD (Fig. 3A-ii, A-iii, respectively) for Alexa 350 dye staining on the three cell lines suggests that, overall, TeCD offers tight and well-separated clusters, which are necessary for use of the FCB technique. Cell detachment (invasive or noninvasive) could hamper the health of specific dye-binding residues in the cells. Alexa and Pacific dyes, typically used for FCB, have succinimidyl ester (NHS ester), and these have specific affinity to amine groups on proteins (22). Preservation of at least those dye binding residues is essential for effective barcoding. Should these residues be damaged/sacrificed during cell detachment, cells in those barcoded samples are expected to exhibit differential uptake of the dye leading to either a bimodal or relatively broader (and therefore overlapping) distribution. This raises a question as to whether significant fraction of all cells treated with a particular dye concentration appear together in a certain distinct, nominal fluorescence range, which, besides suggesting residue preservation is crucial for sample identification post acquisition. In order to address this question, while performing the FCB, for all the cases reported, we used only two-thirds of the single-tube barcoded samples in preparing the *combo-tube*. The remaining one-third was analyzed to test if a particular dye

concentration barcoded sample emitted fluorescence in a detectably different, nominal range *not overlapping* with those for other dye concentrations for the same cell line.

In Figure 3B-i, ii, and iii, the single-tube sample Alexa 350 fluorescence histograms overlaid for the four barcoding dye concentrations (as in Fig. 3A-i, ii, and iii, respectively) for the cell lines detached using the TeCD are contrasted against those obtained in cells detached using AcCD and TrCD. Tight histograms at all dye concentrations considered in the case of cells detached using TeCD suggest that the residues to which Alexa 350 would bind are preserved in all three cell lines having widely different stiffness (Fig. 3B-i). On the contrary, irrespective of the cell stiffness, all three cell lines exposed to accutase resulted in either (A) a bimodal distribution with fluorescence range of one of the modes overlapping with that from samples treated with a different concentration of dye (Fig. 3B-ii: AcCD MCF7) or (B) a broad/left trailing histogram with fluorescence range overlapping, partially or completely, with that for a different dye concentration (Fig. 3B-ii: HeLa, A549). This suggests that even if the barcoded clusters appear well separated, which is the case for accutase-treated HeLa and MCF7 cells barcoded with Alexa 350 (Fig. 3A-ii), the corresponding single-tube histograms clearly show that the FCB thus obtained is unreliable. This is due to the fact that the cells present in these clusters are not directly from the corresponding sample barcoded with the correct signature, that is, dye concentration. While AcCD is

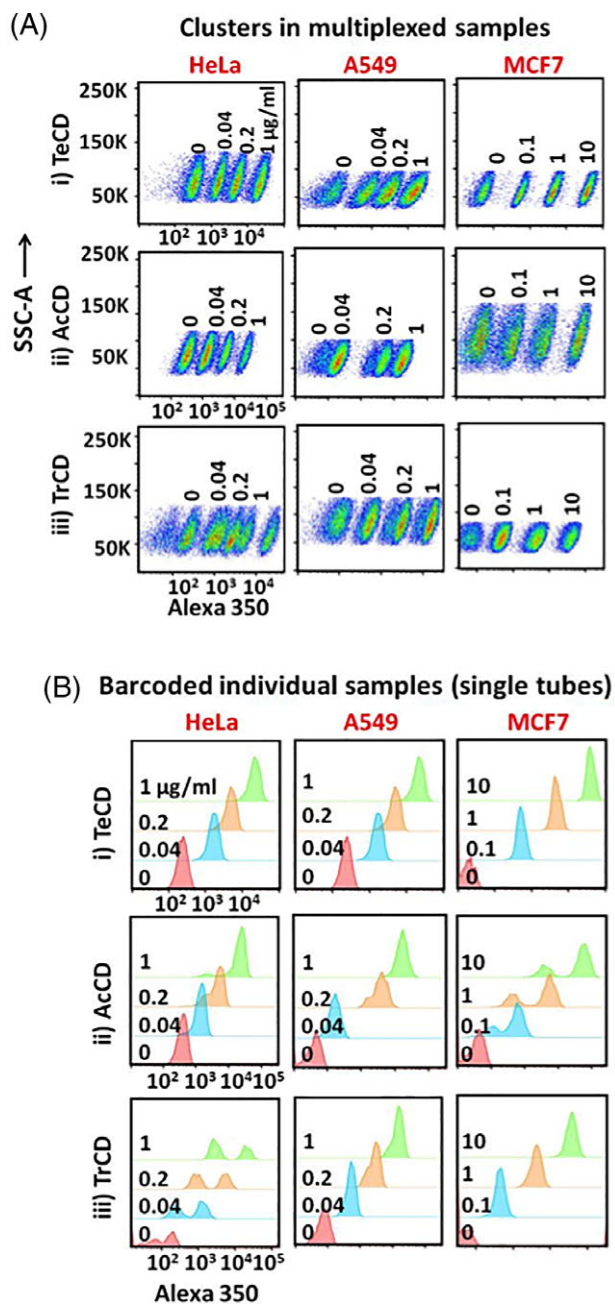


Figure 3. (A) Multiplexing of the three adherent cells by flow cytometry. FCB using Alexa 350 on cells detached by (i) temperature-sensitive method, (ii) accutase treatment, and (iii) standard trypsinization. Different concentrations of Alexa 350 dye (indicated next to each cluster) were used to barcode individual samples. (B) Histograms of the fluorescence from individual samples (single tube) barcoded with different concentrations of Alexa 350 for adherent cells detached using (i) temperature-sensitive method, (ii) accutase treatment, and (iii) trypsinization ($n = 2$). [Color figure can be viewed at wileyonlinelibrary.com]

clearly unsuitable for all three cell lines for FCB, TrCD fails to offer tight clusters only for HeLa (Fig. 3A-iii), which during detachment (at 37 °C) is relatively softer compared to the

other two cell lines as reflected by the mean Young's modulus. Moreover, HeLa cells isolated using TrCD when multiplexed lead to relatively higher cell loss. Thus, TrCD may work for relatively stiffer cells having lower Young's modulus.

Since FCB could be barcoding dye specific, we show in Supporting Information Figure S4 that all three adherent cells isolated using TeCD and barcoded with Alexa 647, whose spectral properties are completely different than that of Alexa 350, can also reliably show well-separated, tight barcoding clusters after multiplexing with each of them aligned with corresponding population from single tubes. Thus, adherent cells detached using temperature-sensitive method can be barcoded using both Alexa 350 and Alexa 647 dyes, which have no spectral overlap, for further increasing the throughput.

Adherent Cells Detached Using TeCD Amenable for High-Throughput Phospho-ERK1/2 Estimation Using FCM

Reliable detection of protein levels in the barcoded samples is the hallmark of utilization of FCB. In this section, we consider the suitability of adherent cells detached using temperature-sensitive method for simultaneous multiplexing of samples and detection of intracellular pERK levels using FCM. For each cell line, we considered three conditions, viz. unstimulated (negative control) and EGF stimulated for 5 and 15 min. These three samples were barcoded with Alexa 350 (Dye1) or Alexa 647 (Dye2) and stained with Alexa 488-tagged pERK antibody ("Materials and methods" section). In particular, based on the barcoding dye concentrations reported in the previous section, we barcoded unstimulated, 5 and 15 min samples, respectively, with low ($\text{Dye1}_L = 0.1 \mu\text{g/ml}$ or $\text{Dye2}_L = 0.02 \mu\text{g/ml}$), medium ($\text{Dye1}_M = 1 \mu\text{g/ml}$ or $\text{Dye2}_M = 0.2 \mu\text{g/ml}$), and high ($\text{Dye1}_H = 10 \mu\text{g/ml}$ or $\text{Dye2}_H = 2 \mu\text{g/ml}$) concentrations of the chosen dye. Post acquisition, the Alexa 350/Alexa 647 channel fluorescence data were first subjected to automated clustering ("Materials and methods" section) to extract individual sample clusters. In addition, simultaneously, intracellular staining of total ERK was carried out for each of these three conditions.

The scatter plot in the planes of Alexa 350 or Alexa 647 fluorescence and side scatter showing the clear separation of the barcoded samples for HeLa and MCF7 cell lines, respectively, is in Figure 4A,B. Histograms corresponding to the three barcoded samples, that is, unstimulated and EGF for 5 and 15 min, comparing the pERK activation levels for these two cell lines are in Figure 4C,D. pERK level in a cell depends on the total ERK in it. In Figure 4E,F, we present the effect of stimulation on the total ERK level distribution for HeLa and MCF7 cells. The total ERK distribution shape and location variation due to stimulation are not significant when compared with the pronounced effect observed on the pERK distribution. (Corresponding barcoding clusters and histograms for A549 are in Supporting Information Figure S5. All observations for HeLa and MCF7 hold for A549 as well except that the pERK activation post stimulation is not as pronounced.)

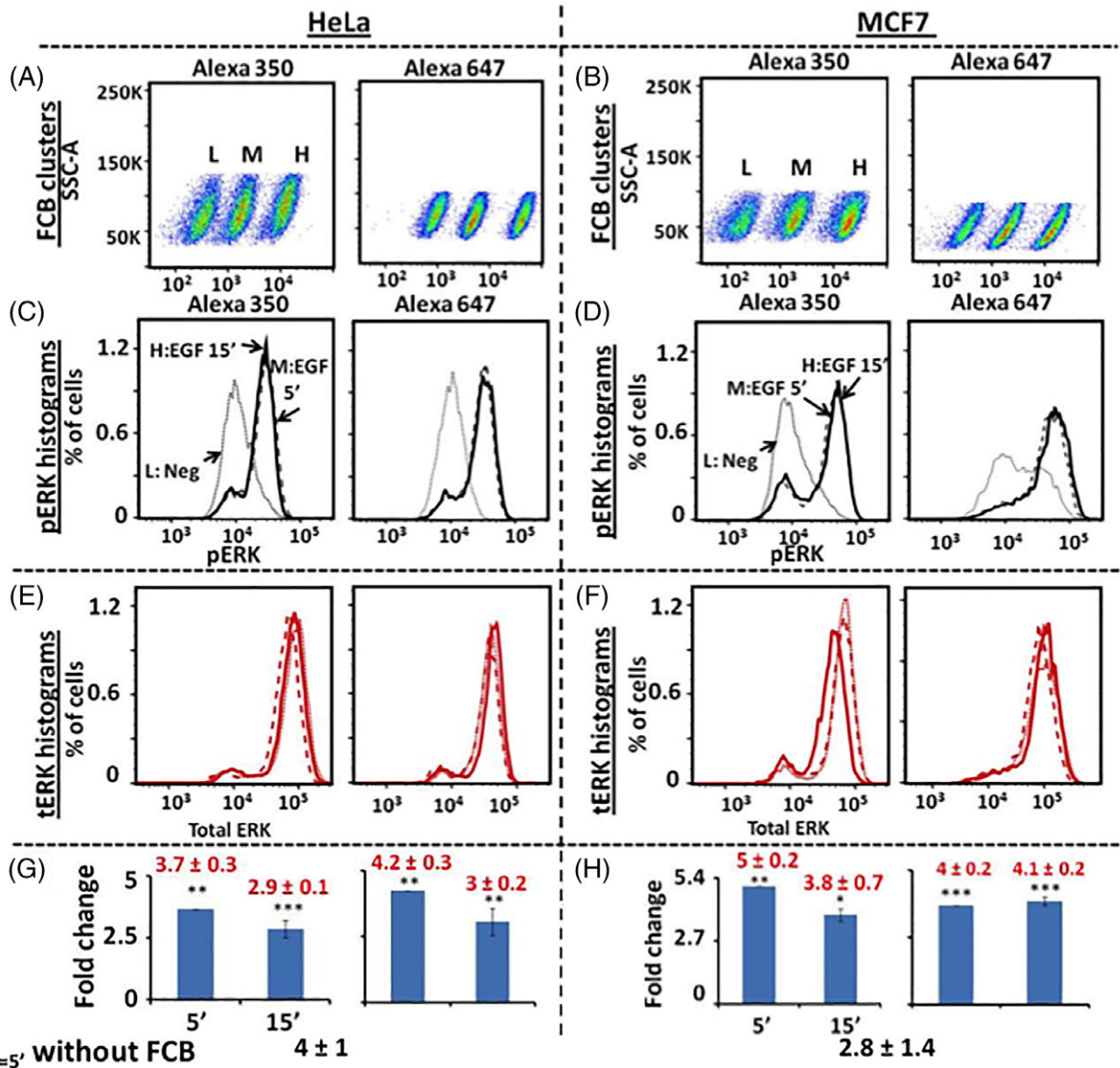


Figure 4. Flow cytometry-based detection of time-dependent pERK levels in EGF stimulated multiplexed (using Alexa 350 or Alexa 647) HeLa (left panel) and MCF7 (right panel) cells detached using temperature-sensitive method. (A and B) Clusters showing three samples barcoded with Alexa 350 or 647. (C and D) pERK histograms for the three conditions viz. negative control (neg—dotted line), 5' stimulation (EGF 5'—dashed line), and 15' stimulation (EGF 15'—solid line) (Neg, EGF 5', and EGF 15', respectively, were barcoded with low [L], medium [M], and high [H] concentrations of the dye) ($n = 3$). Post acquisition, data were subjected to automated gating, deconvolution, and further processing ("Materials and methods" section). (E and F) Total ERK (tERK) histograms for each treatment condition (neg—dotted line, EGF 5'—dashed line, and EGF 15'—solid line) ($n = 2$). (G and H) Fold change, FC_t in pERK levels following EGF 5' or 15' stimulation (Student's paired t -test was performed, $*P < 0.05$, $**P < 0.01$, $***P < 0.001$). $FC_{t=5'}$ without FCB is shown below the bar graphs. Fold change, $FC_t = ([MFI]_{pERK,t} - [MFI]_{pERK,DN}) / ([MFI]_{tERK,t} - [MFI]_{tERK,DN}) / ([MFI]_{pERK,t=0} - [MFI]_{pERK,DN}) / ([MFI]_{tERK,t=0} - [MFI]_{tERK,DN})$, where $[MFI]_{pERK,t}$ and $[MFI]_{tERK,t}$ respectively, are the median fluorescence intensity (MFI) of the pERK distribution and of the tERK distribution for cells stimulated up to time t with $[MFI]_{pERK,DN}$ and $[MFI]_{tERK,DN}$ being corresponding MFI for double negative cells (unstimulated, unstained). Note that $t = 0$ refers to negative control, that is, unstimulated and stained. [Color figure can be viewed at wileyonlinelibrary.com]

In order to compare the pERK levels, as a metric, we define fold change, $FC_t = ([MFI]_{pERK,t} - [MFI]_{pERK,DN}) / ([MFI]_{tERK,t} - [MFI]_{tERK,DN}) / ([MFI]_{pERK,t=0} - [MFI]_{pERK,DN}) / ([MFI]_{tERK,t=0} - [MFI]_{tERK,DN})$, where $[MFI]_{pERK,t}$ and $[MFI]_{tERK,t}$ respectively, are the MFI of the pERK distribution and of the total ERK distribution for cells stimulated up to time t with $[MFI]_{pERK,DN}$ and $[MFI]_{tERK,DN}$ being corresponding

MFI for double negative cells (unstimulated and unstained). Note that $t = 0$ corresponds unstimulated (negative control) case. For the two barcoding dyes considered, $FC_{t=5'}$ and $FC_{t=15'}$ are in Figure 4G,H and Supporting Information Figure S5D, respectively, for HeLa, MCF7, and A549 and that estimated from the histograms (Fig. 2B and Supporting Information Fig. S2B) for the case without barcoding is presented

below corresponding bar charts. (Note that for estimating FC_t without barcoding, the total ERK histograms in Figure 4E,F and Supporting Information Figure S5C were used for scaling.) $FC_t = 5'$ with and without barcoding match well for both HeLa (Fig. 4G) and A549 (Supporting Information Fig. S5D). However, for the case of MCF7, $FC_t = 5'$ with barcoding matches that without barcoding only when the standard deviation across replicates is discounted (Fig. 4H). While HeLa cells displayed a decrease in the FC_t with an increase in stimulation time, A549 cells exposed to EGF for different times had only marginal effect on the FC_t . Moreover, this is similar to that observed for the case of immunoblotting. (Note that FC_t trends obtained by FCM and by western blot are only comparable as the immunoblotting quantitation is protein input loading sensitive (40).) In contrast, for the case of MCF7, pERK FC_t time course obtained when multiplexed with Alexa 350 was marginally different than that achieved when barcoded with Alexa 647.

During barcoding, cells exposed to different concentrations of dye are mixed together in a combo-tube before staining. It is thus necessary to exclude the possibility of a certain dye concentration (barcodes) affecting the pERK levels in cells. In order to assess this, we repeated the complete panel of stimulation, barcoding, intracellular staining, acquisition, clustering, and analysis by flipping the barcodes. Specifically, we barcoded unstimulated, 5 and 15 min samples, respectively with high (Dye1_H = 10 µg/ml or Dye2_H = 2 µg/ml), medium (Dye1_M = 1 µg/ml or Dye2_M = 0.2 µg/ml), and low (Dye1_L = 0.1 µg/ml or Dye2_L = 0.02 µg/ml) concentrations of the chosen dye. The barcoding clusters and histograms along with corresponding FC_t comparing the pERK levels for all three conditions are presented in Supporting Information Figure S6 for all three cell lines. The histograms and the FC_t obtained for the three conditions while using flipped barcodes are similar as that for regular barcoding (Fig.4G,H) for HeLa and MCF7 cell lines. In contrast, for the case of A549, flipped barcoded samples show only marginal activation post stimulation similar to that observed when multiplexed using regular barcodes. This suggests that the barcoding intensity itself will not interfere with the pERK response to EGF stimulation in the three cell lines considered.

While barcoding and intracellular staining was presented for assessing the time course of pERK levels post stimulation, multiplexing of samples is possible for detecting dose-dependent pERK response in short time scales. In Supporting Information Figure S7, we show that pERK levels can be reliably estimated even by multiplexing of samples exposed to different PMA concentrations.

DISCUSSION

Single-cell level detection of intracellular protein markers at short time scales is needed for tracking early signal transduction response. In this study, as a first, we systematically show that adherent cells detached via noninvasive temperature-sensitive detachment method are amenable for reliably combining FCB and intracellular phospho-ERK1/2

level measurement using FCM. Such detached cells can be stimulated post detachment, possibility of which makes the proposed approach directly amenable for short time scale sampling. In particular, we demonstrate effective FCB using two commonly used dyes Alexa 350 and 647 (having no spectral overlap) and FCM-based detection of EGF induced pERK in three adherent cell lines having characteristically different cell stiffness. Demonstration of multiplexing using two spectrally nonoverlapping dyes opens the possibility of increasing the throughput by barcoding the adherent cells with two dyes (22).

Trypsinization and accutase treatment are typical methods for cell detachment. We show that pERK distribution in HeLa, MCF7, or A549 cells detached using any of the three detachment methods, viz., temperature-sensitive (TeCD), accutase treatment (AcCD), and standard trypsinization (TrCD) and then stimulated with EGF is qualitatively similar. TeCD isolated HeLa or MCF7 cells stimulated for 5 min show a pronounced bimodal distribution. For HeLa cells, this is in agreement with that reported by Shindo et al. (5). Our FCM-based measurement of pERK levels thus indicates that temperature-sensitive detachment method may be well-suited for capturing such clear bimodal distributions.

Multiplexing of samples via FCB has several advantages (13). Traditionally, presence of tight clusters corresponding to barcoded cells post acquisition is considered sufficient for the successful implementation of multiplexing via FCB (24). While the presence of well-separated tight clusters is necessary, sufficiency is when all cells exposed to particular barcoding dye concentration appear together in the same tight cluster. For all three cell lines detached using the three methods, we make a systematic, comprehensive comparison of the tight barcoded clusters multiplexed using Alexa 350 (in a combo-tube) with the clusters corresponding to individual samples (as many as the number of barcodes) in single tubes. Adherent cells, whether stiffer or softer under normal culture conditions, when isolated using TeCD and barcoded satisfy both the necessary and sufficient conditions (Fig. 3). This could be due to the fact that the cells considered have comparable stiffness at RT, the temperature at which cells are isolated using TeCD. While cells detached via AcCD upon multiplexing do not satisfy both these conditions simultaneously, TrCD (at 37°C) offering single-cell suspension is suitable for multiplexing only when the cells (MCF7 and A549, Fig. 3A-iii,B-iii) are relatively stiffer in nature.

Detachment of softer cells having higher mean Young's modulus requires relatively harsher enzymatic treatment, which could damage the protein residues (15). This may explain why AcCD or TrCD isolated HeLa cells, in which amine group on protein residues (to which Alexa dyes bind) may have been compromised, do not satisfy the sufficiency condition, thereby making them unsuitable for FCB. However, A549 cells being stiffer with lower Young's modulus require milder trypsin treatment leading to potential preservation of those protein residues to which Alexa dyes bind. Since the detachment via temperature-sensitive method is noninvasive, those Alexa-binding protein residues are likely to be

intact, thereby making the cells isolated by this method suitable for multiplexing via FCB.

Simultaneous FCB and intracellular pERK level detection in all three cell lines detached using TeCD showed conclusively that barcoding does not interfere with pERK response and vice versa. Thus, cells detached using TeCD can be reliably used for high-throughput intracellular phospho-protein measurements using FCM. The approach demonstrated on a few immortalized epithelial cell lines in this study can be extended to other adherent immortalized cells and primary normal and cancerous cells whose elasticity (Young's modulus) at RT (25°C) is in the same range as that of the cells considered. Temperature-sensitive detachment for primary cells has been considered in the recent past (27). Suitability of such cells for multiplexing of samples needs to be investigated further.

ACKNOWLEDGMENTS

FACS Central facility and the Department of Bioscience and Bioengineering Central Instrumentation facility, IIT Bombay, are acknowledged for access. One of the authors (GV) wishes to thank Prof. Sameer Jadhav for many useful discussions. We also thank Dr. Girija Kalantre for helpful discussions. We gratefully acknowledge Prof. Sarika Mehra for access to the SpectraMax M5 plate reader and Prof. Ruchi Anand for access to the 4°C facility. Contributions by Shadik Shaik toward finding the barcoding clusters are acknowledged. Two of the authors (PS and AM) gratefully acknowledge Sunandan Divatia School of Science, NMIMS for permission to conduct their M.Sc full-time-internship at IIT Bombay. We thank the anonymous reviewers for their valuable suggestions.

LITERATURE CITED

- Altschuler SJ, Wu LF. Cellular heterogeneity: When do differences make a difference? *Cell* 2010;141(4):559–563.
- Tellez-Gabriel M, Ory B, Lamoureux F, Heymann M-F, Heymann D. Tumour heterogeneity: The key advantages of single-cell analysis. *Int J Mol Sci* 2016;17(12):2142.
- Cohen AA, Geva-Zatorsky N, Eden E, Frenkel-Morgenstern M, Issaeva I, Sigal A, Milo R, Cohen-Saidon C, Liron Y, Kam Z, et al. Dynamic proteomics of individual cancer cells in response to a drug. *Science* 2008;322:1511–1516.
- Gascoigne KE, Taylor SS. Cancer cells display profound intra- and interline variation following prolonged exposure to antimetabolic drugs. *Cancer Cell* 2008;14:111–122.
- Shindo Y, Iwamoto K, Mouri K, Hibino K, Tomita M, Kosako H, Sako Y, Takahashi K. Conversion of graded phosphorylation into switch-like nuclear translocation via autoregulatory mechanisms in ERK signalling. *Nat Commun* 2016;7:10485.
- Mizrahi O, Shalom EI, Baniyash M, Klieger Y. Quantitative flow cytometry: Concerns and recommendations in clinic and research. *Cytometry Part B: Clin Cytom* 2018;94(2):211–218.
- Kanegane H, Hoshino A, Okano T, Yasumi T, Wada T, Takada H, Okada S, Yamashita M, Yeh TW, Nishikomori R, et al. Flow cytometry-based diagnosis of primary immunodeficiency diseases. *Allergol Int* 2018; 67(1):43–54.
- Irish JM, Hovland R, Krutzik PO, Perez OD, Bruserud O, Gjertsen BT, Nolan GP. Single cell profiling of potentiated phospho-protein networks in cancer cells. *Cell* 2004;118(2):217–228.
- Nolan GP. Flow cytometry in the post fluorescence era. *Best Pract Res Clin Haematol* 2011;24(4):505–508.
- Covey TM, Cesano A. Modulated multiparametric phosphoflow cytometry in hematological malignancies: Technology and clinical applications. *Best Pract Res Clin Haematol* 2010;23(3):319–331.
- Willison KR, Klug DR. Quantitative single cell and single molecule proteomics for clinical studies. *Curr Opin Biotechnol* 2013;24(4):745–751.
- Bendall SC, Nolan GP. From single cells to deep phenotypes in cancer. *Nat Biotechnol* 2012;30(7):639–647.
- Krutzik PO, Nolan GP. Fluorescent cell barcoding in flow cytometry allows high-throughput drug screening and signaling profiling. *Nat Methods* 2006;3(5):361–368.
- Geiler-Samerotte KA, Bauer CR, Li S, Ziv N, Gresham D, Siegal ML. The details in the distributions: Why and how to study phenotypic variability. *Curr Opin Biotechnol* 2013;24(4):752–759.
- Heng BC, Liu H, Ge Z, Cao T. Mechanical dissociation of human embryonic stem cell colonies by manual scraping after collagenase treatment is much more detrimental to cellular viability than is trypsinization with gentle pipetting. *Biotechnol Appl Biochem* 2007;47(Pt 1):33–37.
- Abrahamsen I, Lorens JB. Evaluating extracellular matrix influence on adherent cell signaling by cold trypsin phosphorylation-specific flow cytometry. *BMC Cell Biol* 2013;14(1):36.
- Glazer ES, Massey KL, Curley SA. A protocol to effectively create single cell suspensions of adherent cells for multiparameter high-throughput flow cytometry. *In Vitro Cell Dev Biol Animal* 2010;46:97–101.
- Freshney RI. *Culture of Animal Cells: A Manual of Basic Technique*. 5th ed. Hoboken, NJ: John Wiley & Sons, Inc., 2005.
- Zeng J, Mohammadreza A, Gao W, Merza S, Smith D, Kelbauskas L, Meldrum DR. A minimally invasive method for retrieving single adherent cells of different types from cultures. *Sci Rep* 2014;4:5424.
- Gibbs KD Jr, Gilbert PM, Sachs K, Zhao F, Blau HM, Weissman IL, Nola GP, Majeti R. Single-cell phospho-specific flow cytometric analysis demonstrates biochemical and functional heterogeneity in human hematopoietic stem and progenitor compartments. *Blood* 2011;117(16):4226–4233.
- George AA, Paz H, Fei F, Kirzner J, Kim YM, Heisterkamp N, Abdel-Aziz H. Phosphoflow-based evaluation of Mek Inhibitors as small-molecule therapeutics for B-cell precursor acute lymphoblastic Leukemia. *PLoS One* 2015;10(9):1–17.
- Krutzik PO, Clutter MR, Trejo A, Nolan GP. Fluorescent cell barcoding for multiplex flow cytometry. *Curr Protoc Cytom* 2011;Chapter 6:Unit 6.31.
- Wu S, Jin L, Vence L, Radvanyi LG. Development and application of “phosphoflow” as a tool for immunomonitoring. *Expert Rev Vaccines* 2010;9(6):631–643.
- Cornez I, Joel M, Taskén K, Langmoen IA, Glover JC, Berge T. EGF signalling and rapamycin-mediated mTOR inhibition in glioblastoma multiforme evaluated by phospho-specific flow cytometry. *J Neurooncol* 2013;112(1):49–57.
- Paraiso KH, Van Der Kooi K, Messina JL, Smalley KS. Measurement of constitutive MAPK and PI3K/AKT signaling activity in human cancer cell lines. *Methods Enzymol* 2010;484:549–567.
- Birtwistle MR, Rauch J, Kiyatkin A, Aksamitiene E, Dobrzyński M, Hoek JB, Kolch W, Ogunnaik BA, Kholodenko BN. Emergence of bimodal cell population responses from the interplay between analog single-cell signaling and protein expression noise. *BMC Syst Biol* 2012;6:109.
- Mandal K, Bolland M, Bureau L. Thermoresponsive micropatterned substrates for single cell studies. *PLoS One* 2012;7(5):e37548.
- Nagase K, Kobayashi J, Okano T. Temperature-responsive intelligent interfaces for biomolecular separation and cell sheet engineering. *J R Soc Interface* 2009;6(3):S293–S309.
- Yamato M, Okano T. Cell sheet engineering. *Mater Today* 2004;7(5):42–47.
- Corver WE, Cornelisse CJ, Hermans J, Fleuren GJ. Limited loss of nine tumor-associated surface antigenic determinants after tryptic cell dissociation. *Cytometry* 1995;19(3):267–272.
- Bajpai R, Lesperance J, Kim M, Tersikh AV. Efficient propagation of single cells acetate-dissociated human embryonic stem cells. *Mol Reprod Dev* 2008;75(5):818–827.
- <https://assets.thermofisher.com/TFS-Assets/LCD/Application-Notes/AppNote-Nunc-UpCell-N20230.pdf>. 2008
- Schneider CA, Rasband WS, Eliceiri KW. NIH Image to ImageJ: 25 years of image analysis. *Nat Methods* 2012;9:671–675.
- Ge Y, Sealfon SC. flowPeaks: A fast unsupervised clustering for flow cytometry data via K-means and density peak finding. *Bioinformatics* 2012;28(15):2052–2058.
- Castillo-Hair SM, Sexton JT, Landry BP, Olson EJ, Igoshin OA, Tabor JJ. FlowCal: A user-friendly, open source software tool for automatically converting flow cytometry data from arbitrary to calibrated units. *ACS Synth Biol* 2016;5(7):774–780.
- Li M, Liu L, Xi N, Wang Y, Xiao X, Zhang W. Effects of temperature and cellular interactions on the mechanics and morphology of human cancer cells investigated by atomic force microscopy. *Sci China Life Sci* 2015;58(9):889–901.
- Purvis JE, Lahav G. Encoding and decoding cellular information through signaling dynamics. *Cell* 2013;152(5):945–956.
- Iwamoto N, D'Alessandro LA, Depner S, Hahn B, Kramer BA, Lucarelli P, Vlasov A, Stepath M, Böhm ME, Deharde D, et al. Context-specific flow through the MEK/ERK module produces cell- and ligand-specific patterns of ERK single and double phosphorylation. *Sci Signal* 2016; 9 (413), ra13.
- Chen KD, Li YS, Kim M, Li S, Yuan S, Chien S, Shyy JY. Mechanotransduction in response to shear stress. Roles of receptor tyrosine kinases, integrins, and Shc. *J Biol Chem* 1999;274(26):18393–18400.
- Janes KA. An analysis of critical factors for quantitative immunoblotting. *Sci Signal* 2015;8(371):rs2.